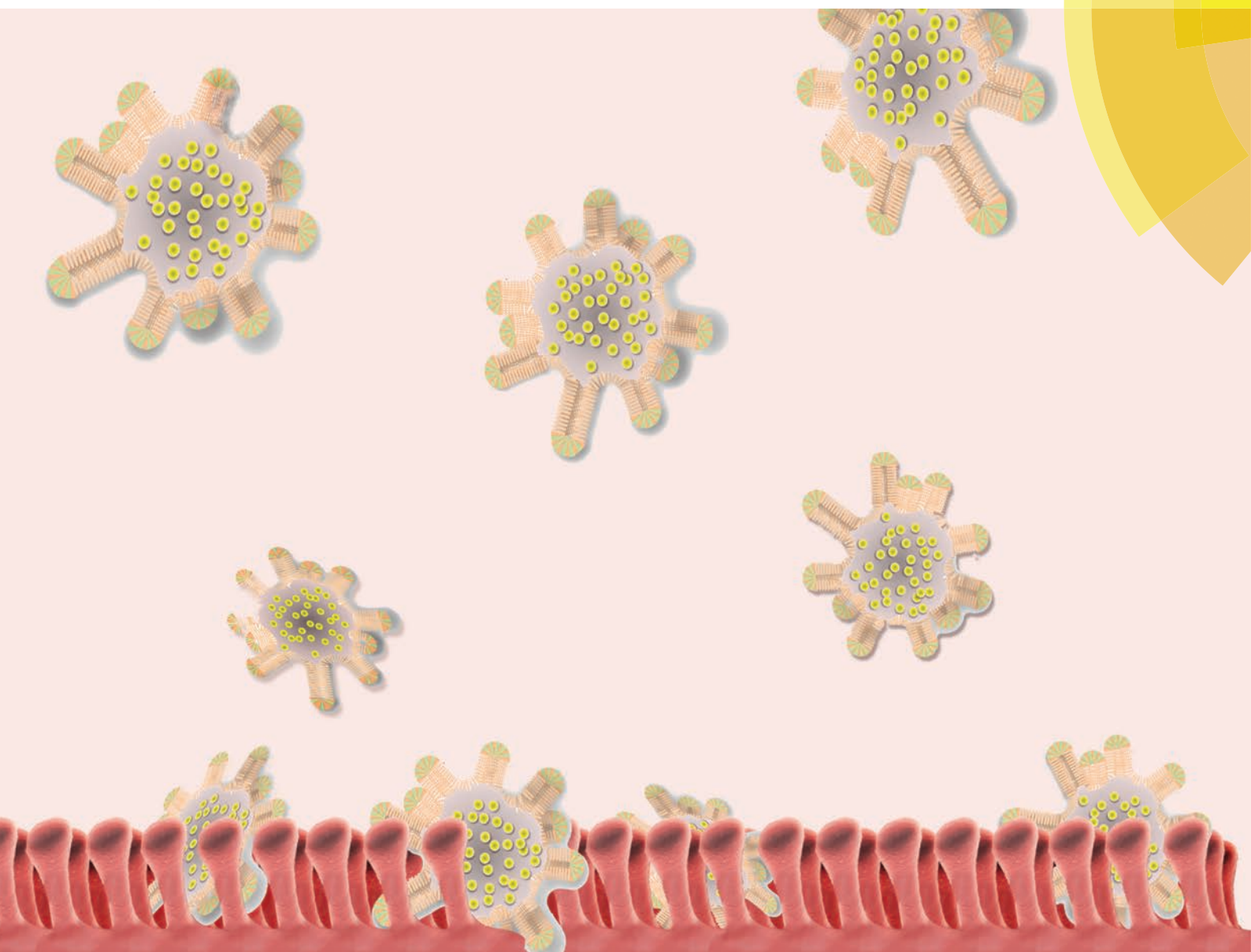


# Nanoscale

[www.rsc.org/nanoscale](http://www.rsc.org/nanoscale)



ISSN 2040-3364



COMMUNICATION  
Qun Wang *et al.*  
An intestinal Trojan horse for gene delivery





## An intestinal Trojan horse for gene delivery

Cite this: *Nanoscale*, 2015, 7, 4354 Haisheng Peng,<sup>a,d</sup> Chao Wang,<sup>b</sup> Xiaoyang Xu,<sup>c</sup> Chenxu Yu<sup>b</sup> and Qun Wang<sup>\*a</sup>

Received 29th October 2014,  
 Accepted 5th January 2015

DOI: 10.1039/c4nr06377e

[www.rsc.org/nanoscale](http://www.rsc.org/nanoscale)

The intestinal epithelium forms an essential element of the mucosal barrier and plays a critical role in the pathophysiological response to different enteric disorders and diseases. As a major enteric dysfunction of the intestinal tract, inflammatory bowel disease is a genetic disease which results from the inappropriate and exaggerated mucosal immune response to the normal constituents in the mucosal microbiota environment. An intestine targeted drug delivery system has unique advantages in the treatment of inflammatory bowel disease. As a new concept in drug delivery, the Trojan horse system with the synergy of nanotechnology and host cells can achieve better therapeutic efficacy in specific diseases. Here, we demonstrated the feasibility of encapsulating DNA-functionalized gold nanoparticles into primary isolated intestinal stem cells to form an intestinal Trojan horse for gene regulation therapy of inflammatory bowel disease. This proof-of-concept intestinal Trojan horse will have a wide variety of applications in the diagnosis and therapy of enteric disorders and diseases.

### 1. Introduction

As the major organ in mammals, the intestine is both a catalytic and absorptive site where most of the chemical digestion and nutrient and drug absorption in the gastrointestinal (GI) tract take place. As the interface of the intestinal tract, the intestinal epithelium forms an essential element of the mucosal barrier and plays a critical role in the pathophysiological response to different enteric disorders and diseases, such

as inflammatory bowel disease (IBD). IBD defines a group of idiopathic inflammatory disorders of the GI tract characterized by chronic and sometimes irreversible impairment of the gastrointestinal structure and function.<sup>1</sup> Pathological factors may trigger IBD by breaking the mucosal barrier, stimulating immune responses, and/or altering the balance between the beneficial and pathogenic enteric bacteria in genetically susceptible individuals.<sup>2</sup> It is believed that IBD is a genetic disease which results from the inappropriate and exaggerated mucosal immune response to the normal constituents in the mucosal microbiota environment.

Drug delivery systems targeting the intestine have unique advantages in the treatment of IBD.<sup>3,4</sup> Their therapeutic efficacy is dependent on the on-site concentration of the drug in the intestinal mucosa.<sup>5</sup> Thus, they are ideal to deliver drugs targeting the inflammation sites of IBD patients to minimize the potential systemic adverse effects. Nanoparticles, which can protect and release conjugated drugs on-site, have shown their ability to accumulate in the inflamed intestinal tissues.<sup>4,6</sup> Previous research has demonstrated the promising potential of nanoparticle-based treatments for IBD.<sup>7,8</sup> However, difficulties in optimizing the adhesion and systemic absorption of nanoparticles have significantly limited their use in the treatment of IBD.<sup>9</sup>

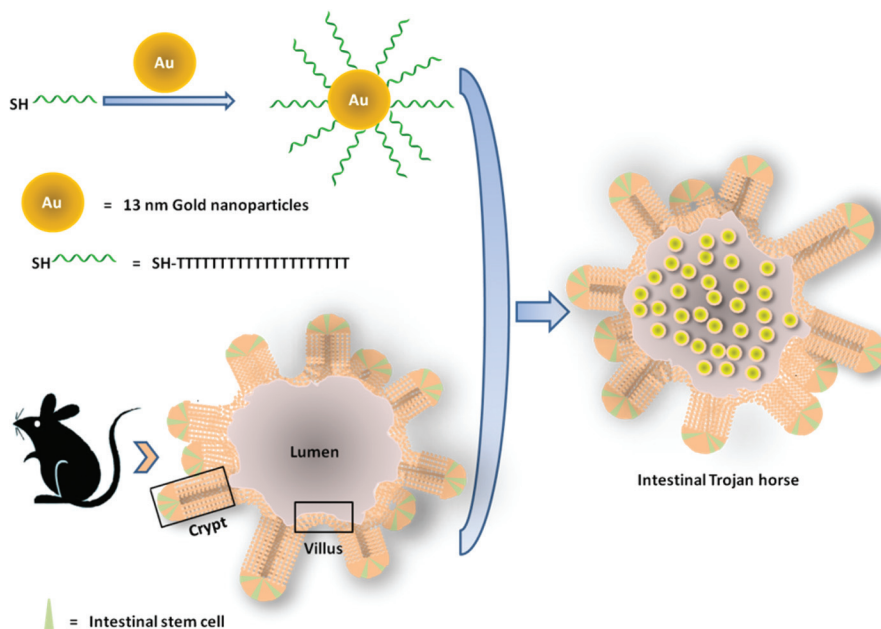
As a new concept in drug delivery, the Trojan horse system with the synergy of nanotechnology and host cells has received intense attention in recent years. The therapeutic nanoparticles can be loaded into host cells *ex vivo* due to endocytosis. Then the nanoparticle encapsulated cell, the “Trojan horse”, could be injected back into the body as a delivery vector for therapeutic purposes.<sup>10,11</sup> The strategy of using the Trojan horse system for drug delivery can achieve improved biodistribution, increased local drug concentration, extended retention time, prolonged dosing intervals, and enhanced therapeutic efficacy. Moreover, Trojan horse using donor cells from recipients may have complicated mechanisms to avoid immune system attack, home to specific tissues, cross impermeable barriers, and modulate their microenvironments. Because of these unique characteristics, Trojan horse is a novel class of

<sup>a</sup>Department of Chemical and Biological Engineering, Iowa State University, Ames, IA 50011, USA. E-mail: [qunwang@iastate.edu](mailto:qunwang@iastate.edu); Fax: +(515) 294-8216; Tel: +(515) 294-4218

<sup>b</sup>Department of Agricultural and Biosystems Engineering, Iowa State University, Ames, IA 50011, USA

<sup>c</sup>Department of Chemical, Biological, and Pharmaceutical Engineering, New Jersey Institute of Technology, Newark, NJ 07102, USA

<sup>d</sup>Department of Pharmaceutics, Daqing Campus, Harbin Medical University, Daqing, 163319, China



**Scheme 1** A novel intestinal "Trojan horse" delivery system employs the synergy of intestinal stem cells and gold nanoparticles for gene delivery.

therapeutics and drug carriers with high specificity and a long period of persistence. However, one big challenge of this Trojan horse strategy is to ensure that the intercellular drug cargos remain inactive and nontoxic to their host cells until the payload has been delivered to the target tissue.

DNA-functionalized gold nanoparticles (GNPs) have been extensively used in biomedicine, in applications such as probes in diagnostic system,<sup>12</sup> and as therapeutic agents for cellular gene regulation.<sup>13</sup> The nontoxic GNPs can act as anti-sense agents to scavenge mRNA within the cells efficiently by their cooperative binding properties,<sup>14</sup> which facilitates the endocytosis.<sup>15</sup> The dense packing of DNA of the shell on DNA-functionalized GNPs also facilitates the dispersion of nanoparticles in cell culture medium with high salt and serum concentration. This property of DNA-functionalized GNPs plays a critical role in the inhibition of enzymatic nucleic acid degradation.<sup>16</sup> Furthermore, due to the high prevalence of positively charged proteins in the inflamed intestines,<sup>17</sup> DNA-functionalized GNPs with a negative surface charge may more easily adhere to denuded mucosa. All these features of DNA-functionalized GNPs make them excellent candidates to be encapsulated within host cells as a Trojan horse for efficient gene regulation therapies of IBD.

Stem cell therapy using live stem cells to treat diseases is a rapidly growing area of translational medicine. Stem cell originated drug delivery systems have been actively explored thanks to their advantages over synthetic drug delivery systems.<sup>18–21</sup> Their success depends on the appropriate control of the fate and function of stem cells. Enhanced survivability, proliferation, and differentiation of donor cells are desirable for therapeutic applications. Due to the recent advancements in the identification of specific adult stem cells, an *in vitro* model of

intestinal stem cells (ISCs) has been designed.<sup>22</sup> As the cell of origin, single intestinal stem cell can build a crypt–villus structure of the intestinal epithelium *in vitro*.<sup>23</sup> The self-renewing intestinal organoids could be established by a well-defined set of growth factors with uniform presentation.<sup>23</sup> The isolated ISCs autonomously generate a multicellular architecture in a highly stereotypical fashion which is reminiscent of the normal intestine. Therefore, ISCs have great potential in the field of intestinal therapeutics. This self-renewed intestinal "organoid" can be used to treat enteric disorders and diseases, such as intestinal infection, radiation injury, and IBD.<sup>22,24</sup> They are also good candidates as cell hosts to compose an intestinal Trojan horse delivery system.

In the current study, we isolated primary ISCs from mice and expanded them *ex vivo*. The harvested ISCs dramatically grew into cauliflower-like organoid structures that contained large numbers of separate crypts. These intestinal organoids developed the correct overall multicellular mucosal architecture with both Paneth cells and stem cells contained within the structures. When the ISCs were incubated with DNA-functionalized GNPs, the intestinal organoids encapsulated the nanoparticles within the lumen to form a Trojan horse. This proof-of-concept intestinal Trojan horse demonstrated the feasibility of gene regulation therapies for IBD. We believe that this work explores the design and manufacture of ISC originated drug delivery systems. This intestine specific Trojan horse platform will have a wide variety of applications in the diagnosis and therapy for the treatment of enteric disorders and diseases. As shown in Scheme 1, a rationally designed intestinal "Trojan horse" delivery system using a combination of ISCs and nanoparticles offers a novel and potentially advantageous approach to treat IBD.

## 2. Materials and methods

### 2.1. Materials

All materials and solvents were purchased from Life Technologies and used without further purification unless otherwise stated. Matrigel was purchased from Corning Inc. Growth factors EGF, Noggin and R-spondin-1 were purchased from PeproTech Inc. Nanopure™ water (18 MegaOhm; Barnstead International) was used in all experiments and to prepare buffers. The DNA strands were purchased from Integrated DNA Technologies, Inc., and purified by HPLC prior to use.

### 2.2. Preparation of gold nanoparticles

The 13 nm GNPs were synthesized and functionalized with oligonucleotides according to previously reported methods.<sup>25,26</sup> Briefly, 13 nm diameter GNPs were prepared by the citrate reduction of HAuCl<sub>4</sub>. An aqueous solution of HAuCl<sub>4</sub> (1 mM, 500 mL) was brought to a reflux in a 3-neck round bottom glass flask while stirring, and then 50 mL of a 38.8 mM trisodium citrate solution was added quickly, which resulted in a change in the color of the solution from light yellow to dark red. The solution was refluxed for an additional 15 minutes, cooled to room temperature, and subsequently filtered through a 0.45 μm nylon filter (Micron Separations Inc.).

### 2.3. Preparation of DNA-functionalized gold nanoparticles

The oligonucleotide used to functionalize the GNPs was thiol labeled DNA (SH-TTT TTT TTT TTT). The oligonucleotide was purified by reverse-phase high-performance liquid chromatography (RP-HPLC). Prior to use, the disulfide functionality on the oligonucleotides was cleaved by the addition of DTT to lyophilized DNA and the resulting mixture was incubated at room temperature for 1 h (0.1 M DTT, 0.18 M phosphate buffer (PB), pH 8.0). The cleaved oligonucleotides were purified using a NAP-5 column. Freshly cleaved oligonucleotides were added to GNPs (1 OD per 1 mL), and the concentrations of PB and sodium dodecyl sulfate (SDS) were brought to 0.01 M and 0.01%, respectively. The salting process was followed by incubation overnight at room temperature. The solution was brought to 0.1 M NaCl, 10 mM phosphate buffer (pH 7) and allowed to stand overnight. To remove excess oligonucleotides, the GNPs were centrifuged and the supernatant was removed, leaving a pellet of GNPs at the bottom. The particles were then resuspended in a buffer (0.1 M NaCl, 10 mM phosphate buffer, 0.01% SDS pH = 7.0). This washing process was repeated three times.

### 2.4. Isolation of primary ISCs

The primary ISCs within the intestinal crypts were isolated from the proximal half of the mouse small intestine. The intestine specimen which was harvested from the C57BL/6 (B6) mouse was kindly donated by Professor Albert Jergens at the College of Veterinary Medicine of Iowa State University. All animal procedures were conducted with the approval of the Iowa State University Institutional Animal Care and Use Committee.

The mouse small intestine was opened longitudinally and then washed with ice-cold PBS until most of the luminal contents were cleared. The intestinal tissue was cut into 2–4 mm pieces with scissors and transferred to a 50 ml falcon tube. 30 ml ice-cold PBS was added to the tube and the fragments were gently washed up and down using a 10 ml pipette. After the intestinal tissue fragments settled down, the supernatant was discarded. This step was repeated 5–10 times until the supernatant was almost clear. 30 ml ice-cold 2 mM EDTA PBS buffer was added to the 50 ml falcon tube and the tube was gently rocked at 4 °C for 30 minutes. After the intestinal fragments settled down, the supernatant was removed.

Then, 20 ml ice-cold PBS was added to the tube and the fragments were gently washed up and down using a 10 ml pipette. After settling the fragments down, the supernatants were inspected to see whether they were enriched with villi or crypts by inverted microscopy. This procedure was repeated several times until most crypts were released. Then the crypt fractions were passed through a 70 μm cell strainer (Corning Inc.) and collected into a BSA coated 50 ml falcon tube. The villous fractions left on the strainer were discarded. The crypt fractions were centrifuged at 300g for 5 minutes to obtain a cell pellet. The pellet was then re-suspended with a 10 ml ice-cold basal culture medium and transferred into a BSA coated 15 ml falcon tube. The tube was centrifuged again at 150g for 2 minutes to remove single cells. This washing step was repeated 2–3 times until most single cells were removed. After all the washing steps were completed, the number of crypts was counted under an inverted microscope. The harvested primary intestinal crypts were stored in an ice-cold basal culture medium and held on ice for later use.

### 2.5. Preparation of ISC culture solution

The basal culture medium was prepared using Advanced DMEM/F12 supplemented with 2 mM GlutaMax, 10 mM Hepes, and 100 U ml<sup>-1</sup> penicillin/100 μg ml<sup>-1</sup> streptomycin. The obtained basal culture medium was then homogeneously mixed with N2 supplement (1×), B27 supplement (1×), 1 mM *N*-acetylcysteine, 1 μg ml<sup>-1</sup> R-spondin-1, 100 ng ml<sup>-1</sup> Noggin, and 50 ng ml<sup>-1</sup> EGF to form a complete ISC culture medium for future use.

### 2.6. Preparation of the intestinal Trojan horse

10 000 isolated intestinal crypts were added to 1 ml Matrigel and re-suspended. 200 μl of the above cell encapsulated Matrigel was applied in a pre-warmed 48-well Falcon plate (Corning Inc.). The gel was applied on the center of the well so that it could form a flat shape. The plate was then transferred to an incubator and allowed to undergo gelation at 37 °C for 30 minutes. Finally, the 500 μl complete ISC culture medium with growth factors was added to each well and the cell encapsulated gels were cultured in the CO<sub>2</sub> incubator at 37 °C. After 24 hours, DNA-functionalized GNPs at a DNA strand concentration of 100 nM were added directly to the cell culture medium. After another 24 hours, the culture medium was changed with complete ISC culture medium and further



changed every other day. The ISC culture without the treatment of DNA-functionalized GNPs was used as the control. The images of intestinal organoids in gels were recorded using a Nikon Eclipse 2000 inverted microscope.

### 2.7. Viability assessment of the intestinal Trojan horse

For whole-mount viability assessment, an intestinal Trojan horse was released from Matrigel by mechanical force using a p1000 pipette. Then, the intestinal Trojan horse was transferred into Eppendorf tubes. For cell viability assessment, organoids were washed with sterile PBS three times and then incubated for 45 minutes at room temperature with 2  $\mu$ M calcein-AM and 4  $\mu$ M EthD-1 added with PBS. After incubation, these constructs were washed again with PBS in preparation for fluorescence microscopy.

## 3. Results and discussion

### 3.1. Characterization of DNA-functionalized GNPs

The conjugation of DNA to the gold nanoparticles was characterized *via* various methods. UV-Vis spectra of GNPs (Lambda 750, Perkin Elmer, Waltham, MA) before/after DNA conjugation are shown in Fig. 1A. The red-shift of the plasmonic

peak from 519 nm to 536 nm indicated the conjugation of thiolated DNAs onto the GNP surfaces. The TEM image (Jeol 2100, Jeol Ltd, Tokyo, Japan) of the negatively-stained (with 1% uranyl acetate) DNA-GNP complexes is shown in Fig. 1B, also indicating the conjugation of thiolated DNAs to the nanoparticles. Fig. 1C and 1D show the uncoated GNPs and the negatively-stained uncoated GNPs, respectively. As we know, uranyl acetate (UA) could produce high electron density by interaction with lipids/proteins/nucleic acid phosphate groups. Therefore, UA is commonly used as a contrast enhancer of organic molecules in electron microscope measurement. The negatively stained TEM image of DNA-GNP (Fig. 1B) revealed that the thickness of the DNA layer around nanoparticles was approximately 1 nm, manifested by the UA staining as a bright ring. However, in the negatively stained uncoated GNP control TEM image (Fig. 1D), the contrast was weak and the observation of the bright ring was obscure. It was considered that no organic materials surrounded the GNPs and therefore not enough UA was absorbed around GNPs due to the lack of reaction between nucleic acid and UA.

The zeta potential of the GNPs before/after DNA conjugation was measured (Malvern Nano ZS Zetasizer), and the results are shown in Table 1. The changes in zeta potential at the gold nanoparticle surfaces suggested that the net charges

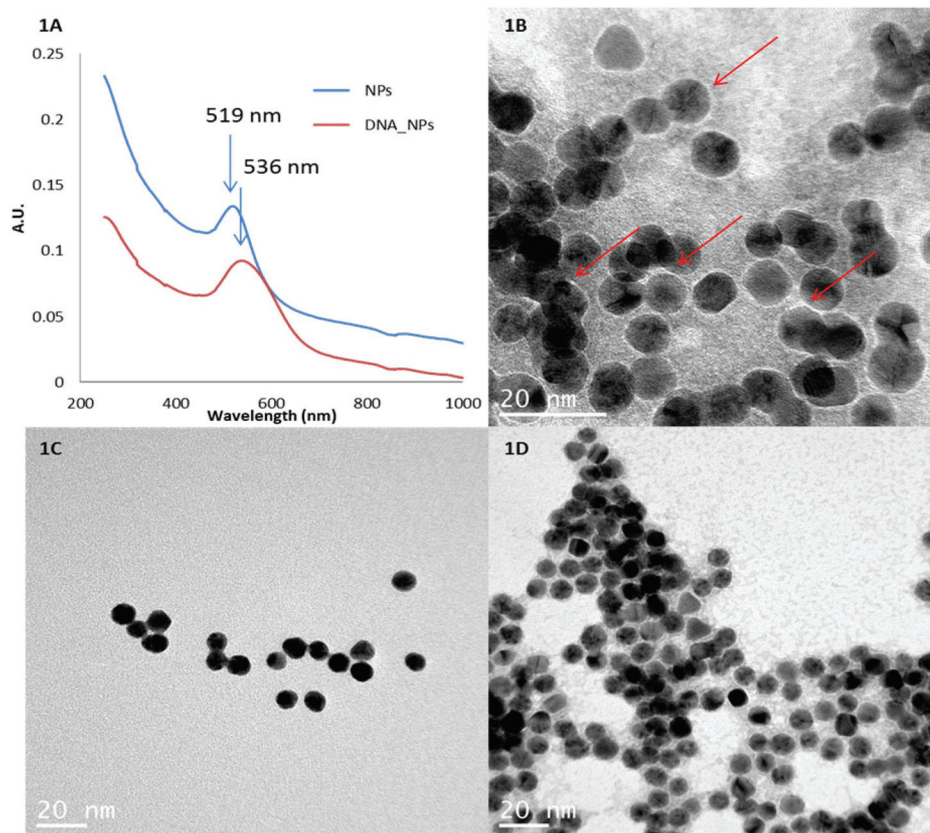


**Fig. 1** Characterization of DNA-GNP conjugation. (A) UV-Vis spectra of GNP before/after DNA conjugation, showing red shift of plasmonic peak by 17 nm; (B) TEM image of GNP-DNA complexes, arrow pointing to surface-conjugated DNA layers illustrated by negative staining with 1% uranyl acetate; (C) TEM image of naked GNP; (D) TEM image of GNP control illustrated by negative staining with 1% uranyl acetate.

**Table 1** Zeta potential measurement showing the addition of negative charges to GNP surfaces due to DNA-conjugation

Particles	Zeta potential (mV)	Mob ( $\mu\text{m cm V}^{-1} \text{s}^{-1}$ )	Cond ( $\text{mS cm}^{-1}$ )
GNP	-16.5	-1.29	0.0836
0.01% SDS	-7.0	-0.549	0.173
GNP-control (0.01% SDS)	-4.33	-0.339	0.0735
GNP-DNA (0.01% SDS)	-26.6	-2.089	0.248

on the particles were changed due to the conjugation of DNAs, which was consistent with the negative charges associated with the DNA backbones. The mobility and conductivity of DNA-GNPs were higher than that of uncoated GNPs. This further confirmed the conjugation of negatively charged DNAs on the GNPs.

### 3.2. Growth of primary ISCs *ex vivo*

As the control, the isolated primary ISCs were cultured in Matrigel without GNPs treatment for 7 days. The *ex vivo* culture system was stable and supported the proliferation and differentiation of ISCs. They expanded and formed organoid structures in which the epithelial cells formed a monolayer at the organoid–gel interface and the extruded cells comprised the lumen. Fig. 2 shows the change of morphology of ISCs cultured in Matrigel over 7 days. The isolated primary ISCs received signals from the growth factors in culture medium and constructed a self-organizing and continuously expanding epithelial organoid structure reminiscent of a normal intestine. These intestinal organoids autonomously generated

asymmetry in a highly stereotypical fashion which led to the rapid formation of crypt-like structures. These crypt-like structures fed into luminal domains where apoptotic cells pinched off into the lumen to constitute the renewing process. These self-renewing intestinal organoids were perfect candidates as cell hosts to compose an intestinal Trojan horse for drug delivery.

### 3.3. Growth of the intestinal Trojan horse *ex vivo*

For a Trojan horse system, the cell internalization and sustained retention of nanoparticles in the host cell play critical roles in determining the therapeutic effects. As DNA-functionalized GNPs can effectively enter cells without the use of transfection reagents,<sup>27</sup> we chose DNA-functionalized GNPs as the delivery vehicle to produce the intestinal Trojan horse.

*In vitro*, the color of DNA-functionalized GNPs was dark red due to the plasmon resonance of the nanoparticles around 520 nm. The encapsulation capability of ISCs to DNA-functionalized GNPs was investigated using a Nikon Eclipse 2000 inverted microscope. As shown in Fig. 3, the nanoparticles were successfully internalized by the intestinal organoids. The DNA-functionalized GNPs in the culture medium penetrated the intestinal crypts and epithelium, and then accumulated in the intestinal lumen. The GNPs sustained in the intestinal lumen up to 7 days and showed a negligible effect on the growth of the intestinal organoids, compared with the cell culture without the treatment of GNPs.

To further test the feasibility of DNA-functionalized GNPs as a carrier for the production of the intestinal Trojan horse, the whole-mount viability assessment of the intestinal Trojan

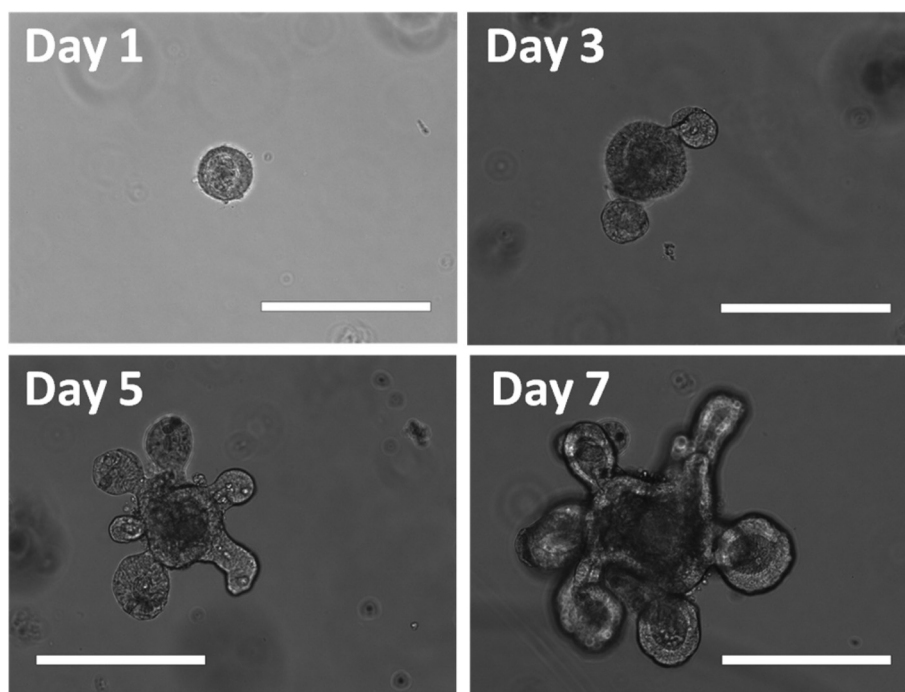


**Fig. 2** The morphology of intestinal stem cells cultured in Matrigel during 7 days. The scale bars were 200  $\mu\text{m}$ .

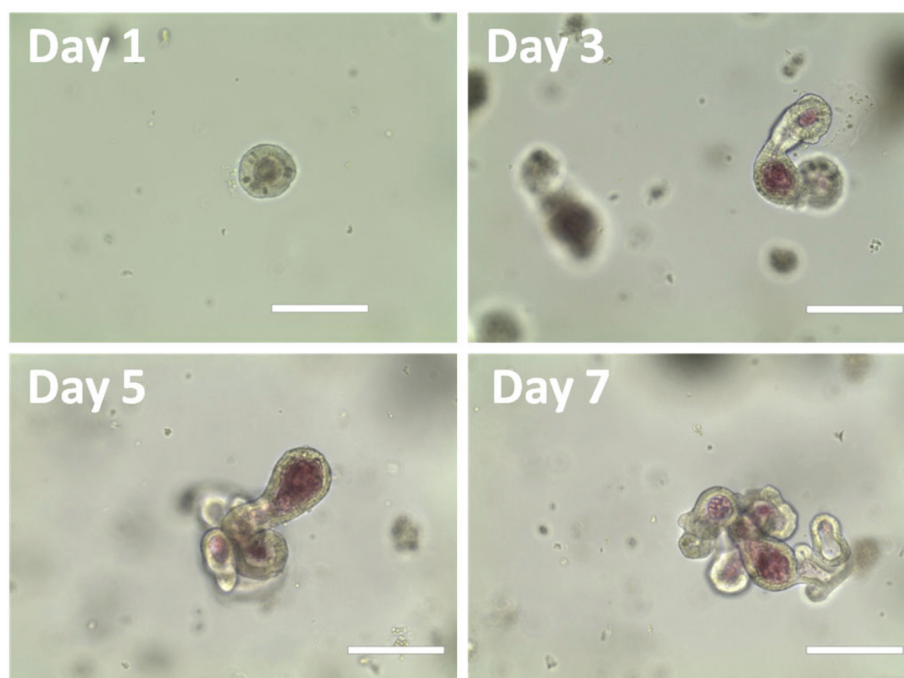


Fig. 3 The morphology of intestinal Trojan horse cultured in Matrigel during 7 days. The scale bars were 200  $\mu\text{m}$ .

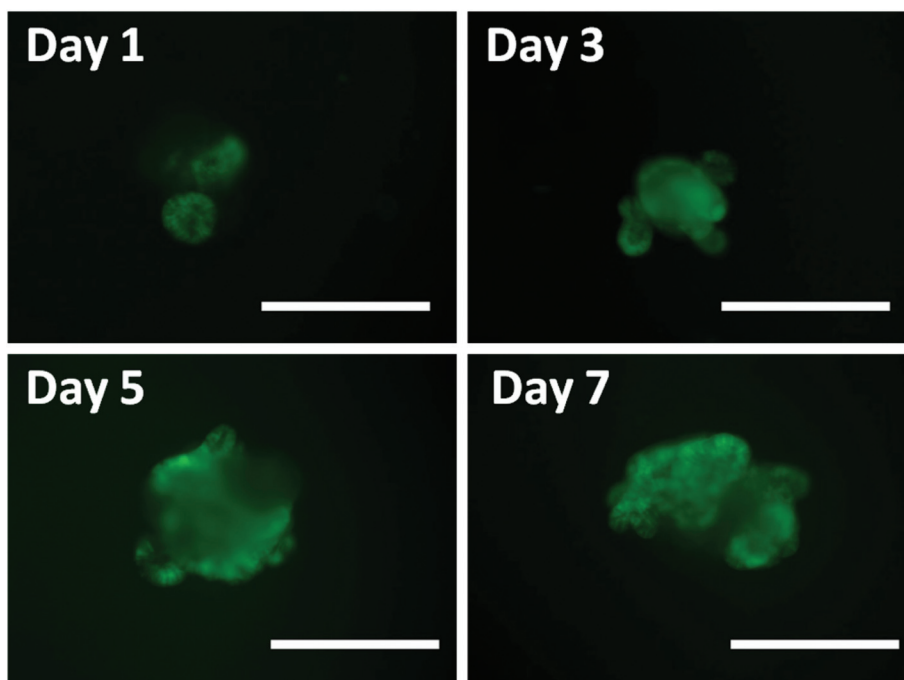


Fig. 4 The live/dead images of intestinal Trojan horse cultured in Matrigel during 7 days. The scale bars were 200  $\mu\text{m}$ .

horse was performed. Fig. 4 showed that the intestinal organoids loaded with DNA-functionalized GNPs were viable and robust over the 7 day period. The encapsulated nanoparticles generated an insignificant cytotoxic profile within the intestinal organoids even after 7 days of incubation. Moreover, the

nanoparticle mediated cell delivery system may overcome the cellular cross resistance of a bunch of therapeutic agents. These pilot results indicated the feasibility of DNA-functionalized GNPs as a gene carrier for the intestinal Trojan horse for the therapy of IBD patients.



## 4. Conclusions

The application of nanotechnology in treating gastrointestinal diseases remains challenging due to the harsh physiological environment in the GI tract. The majority of the current intestinal targeting nanocarriers have limited stability and therefore, unsatisfactory efficacy. The Trojan horse system with the synergy of nanotechnology and host cells can achieve better therapeutic efficacy for specific diseases.

In this proof-of-concept study, a novel intestinal Trojan horse was developed for gene delivery. We demonstrated the feasibility of encapsulating DNA-functionalized GNPs into primary isolated intestinal stem cells to form a Trojan horse for gene regulation therapies for IBD. In future experiments, GNPs with different surface chemistries of different sizes will be synthesized and used to make the intestinal Trojan horse. The effects of surface coating and particle size on encapsulation efficiency and retention time will be investigated. Although we focused on gene delivery, the intestinal Trojan horse delivery system could be extended to carry other cargos, such as peptides, growth factors, plasmids, siRNAs, small chemicals, image agents, and even metallic and atomic substances. This intestinal Trojan horse will have a wide variety of applications in the diagnosis and therapy of enteric disorders and diseases.

## Acknowledgements

This study was supported by Iowa State University (ISU) President's Initiative on Interdisciplinary Research (PIIR) program, Cyclone Research Partnership Grant and McGee-Wagner Interdisciplinary Research Foundation.

## References

- 1 D. K. Podolsky, *N. Engl. J. Med.*, 1991, **325**, 928–937.
- 2 R. B. Sartor, *Nat. Clin. Pract. Gastroenterol. Hepatol.*, 2006, **3**, 390–407.
- 3 D. R. Friend, *Adv. Drug Delivery Rev.*, 2005, **57**, 247–265.
- 4 A. Lamprecht, N. Ubrich, H. Yamamoto, U. Schäfer, H. Takeuchi, P. Maincent, Y. Kawashima and C.-M. Lehr, *J. Pharmacol. Exp. Ther.*, 2001, **299**, 775–781.
- 5 U. Klotz and M. Schwab, *Adv. Drug Delivery Rev.*, 2005, **57**, 267–279.
- 6 Y. Meissner, Y. Pellequer and A. Lamprecht, *Int. J. Pharm.*, 2006, **316**, 138–143.
- 7 A. Lamprecht, H. Yamamoto, H. Takeuchi and Y. Kawashima, *J. Pharmacol. Exp. Ther.*, 2005, **315**, 196–202.
- 8 B. Moulari, D. Pertuit, Y. Pellequer and A. Lamprecht, *Bio-materials*, 2008, **29**, 4554–4560.
- 9 A. Lamprecht, *Nat. Rev. Gastroenterol. Hepatol.*, 2010, **7**, 311–312.
- 10 M.-R. Choi, K. J. Stanton-Maxey, J. K. Stanley, C. S. Levin, R. Bardhan, D. Akin, S. Badve, J. Sturgis, J. P. Robinson and R. Bashir, *Nano Lett.*, 2007, **7**, 3759–3765.
- 11 C.-H. Wu, C. Cao, J. H. Kim, C.-H. Hsu, H. J. Wanebo, W. D. Bowen, J. Xu and J. Marshall, *Nano Lett.*, 2012, **12**, 5475–5480.
- 12 N. L. Rosi and C. A. Mirkin, *Chem. Rev.*, 2005, **105**, 1547–1562.
- 13 N. L. Rosi, D. A. Giljohann, C. S. Thaxton, A. K. Lytton-Jean, M. S. Han and C. A. Mirkin, *Science*, 2006, **312**, 1027–1030.
- 14 A. K. Lytton-Jean and C. A. Mirkin, *J. Am. Chem. Soc.*, 2005, **127**, 12754–12755.
- 15 D. A. Giljohann, D. S. Seferos, P. C. Patel, J. E. Millstone, N. L. Rosi and C. A. Mirkin, *Nano Lett.*, 2007, **7**, 3818–3821.
- 16 D. S. Seferos, A. E. Prigodich, D. A. Giljohann, P. C. Patel and C. A. Mirkin, *Nano Lett.*, 2008, **9**, 308–311.
- 17 A. Dahan, G. L. Amidon and E. M. Zimmermann, *Expert Rev. Clin. Immunol.*, 2010, **6**, 543–550.
- 18 C. D. Porada and G. Almeida-Porada, *Adv. Drug Delivery Rev.*, 2010, **62**, 1156–1166.
- 19 A. U. Ahmed, N. G. Alexiades and M. S. Lesniak, *Curr. Opin. Mol. Ther.*, 2010, **12**, 546.
- 20 F.-J. Müller, E. Y. Snyder and J. F. Loring, *Nat. Rev. Neurosci.*, 2006, **7**, 75–84.
- 21 C. Tang, P. J. Russell, R. Martiniello-Wilks, J. Rasko, E. John and A. Khatri, *Stem Cells*, 2010, **28**, 1686–1702.
- 22 D. H. Scoville, T. Sato, X. C. He and L. Li, *Gastroenterology*, 2008, **134**, 849–864.
- 23 T. Sato, R. G. Vries, H. J. Snippert, M. van de Wetering, N. Barker, D. E. Stange, J. H. van Es, A. Abo, P. Kujala and P. J. Peters, *Nature*, 2009, **459**, 262–265.
- 24 A. S. Gulati, S. A. Ochsner and S. J. Henning, *Am. J. Physiol. Gastrointest. Liver Physiol.*, 2008, **294**, G286–G294.
- 25 J. J. Storhoff, R. Elghanian, R. C. Mucic, C. A. Mirkin and R. L. Letsinger, *J. Am. Chem. Soc.*, 1998, **120**, 1959–1964.
- 26 S. J. Hurst, A. K. Lytton-Jean and C. A. Mirkin, *Anal. Chem.*, 2006, **78**, 8313–8318.
- 27 D. A. Giljohann, D. S. Seferos, W. L. Daniel, M. D. Massich, P. C. Patel and C. A. Mirkin, *Angew. Chem., Int. Ed.*, 2010, **49**, 3280–3294.